RSC Advances

PAPER

View Article Online
View Journal | View Issue

Cite this: *RSC Adv.*, 2017, **7**, 50844

Synthesis and retention properties of molecularly imprinted polymers for antibiotics containing a 5-nitrofuran ring†

Edina Rusen,[a] Aurel Diacon,[a] Alexandra Mocanu,[a] Florica Rizea,[a] Bogdan Bucur,*[b] Madalina Petruta Bucur,[b] Gabriel-Lucian Radu,[b] Elena Bacalum,[c] Mihaela Cheregi[d] and Victor David[d]

Novel molecularly imprinted polymers (MIPs) designated for the solid-phase extraction of antibiotics containing a 5-nitrofuran ring (nitrofurantoin and furaltadone) are reported. The synthesis of these MIPs was based on commercial monomers and cross-linking agents capable of forming hydrogen bonds with the template molecules. Thus, the designed MIPs should involve acceptable costs and easier accessibility. Their retention properties were studied by solid-phase extraction (SPE) procedures and the breakthrough curves were evaluated for both imprinted and non-imprinted polymers (NIPs). Due to the presence of adsorption sites created in polymers by imprinting, the MIPs showed a significant difference in the retention property in comparison to NIPs. The MIPs were also immobilized onto a gold electrode surface by entrapment into a silane sol–gel matrix for the development of a sensor based on electrochemical impedance measurements. The good mechanical adherence of the sol–gel matrix on the gold electrode surface was achieved by formation of a self-assembled monolayer using 3-mercaptopropyl trimethoxisilane that acts as an anchoring bridge.

Received 13th September 2017
Accepted 26th October 2017

DOI: 10.1039/c7ra10196a

rsc.li/rsc-advances

Introduction

Furazolidone (FZD), furaltadone (FTD), nitrofurantoin (NFT) and nitrofurazone (NFZ) belong to the class of synthetic broad spectrum antibiotics, containing a characteristic 5-nitrofuran ring, which have been employed as feed additives for growth promotion, and mainly used for livestock aquaculture and bee colonies in the prophylactic and therapeutic treatment of bacterial and protozoan infections.[1] Nitrofuran antibiotics, employed for the treatment of bacterial diseases in livestock production, were banned from use in the European Union (EU) and in numerous other countries due to concerns about the carcinogenicity of their residues in edible tissue or the threat of development of pathogens with antibiotic resistance.[1] The nitrofuran drugs are available for veterinary and human therapies, only the use for livestock production is prohibited.[2–5] The presence of nitrofuran antibiotic in food still continue to be of international concern, which are metabolized and transformed in chemical species, such as 3-amino-2-oxazolidinone (AOZ), 3-amino-5-morpholinomethyl-2-oxazolidone (AMOZ), semicarbazide (SEM) or 1-aminohydantoin (AHD).[6] European Food Safety Agency (EFSA), has recently provided a scientific opinion on the risks to human health related to the presence of nitrofurans in food by taking 1.0 μg kg^{-1} as possible concentration in which a single nitrofuran marker metabolite is present in foods of animal origin due to insufficient data from monitoring.[7] An indication of the continuous violations is provided by the European Rapid Alert System for Food and Feed (RASFF)[8] online database that contains more than 800 notifications since 2002.[7] The interest in researching the accumulation of these drugs or their metabolites in different animal tissues as well as on the analytical methods for their identification and determination is still actual concern.[9,10] Comparative new studies focused on the interaction of some nitrofuran antibiotics with bovine serum albumin by means of fluorescence and FT-IR spectroscopy, circular dichroism, atomic force microscopy and molecular docking investigation showed that the conformation of bovine serum albumin can be changed and unfolded in the presence of nitrofurans.[11]

The nitrofuran antibiotics determination in various matrices can be performed by diverse chromatographic techniques,[12] which usually require a sample preparation step in order to

[a]*University Politehnica of Bucharest, Faculty of Applied Chemistry and Materials Science, Dept. Bioresources and Polymers Science, 1-7 Gh Polizu, Bucharest 011061, Romania*

[b]*Centre of Bioanalysis, National Institute of Research and Development of Biological Sciences, 296, Splaiul Independentei, Bucharest, 060031, Romania. E-mail: bucurica@yahoo.com; Tel: +40-021-22-00-900*

[c]*University of Bucharest, Research Institute – ICUB, Blvd. M. Kogalniceanu, No. 36-46, Bucharest, 050107, Romania*

[d]*University of Bucharest, Faculty of Chemistry, Department of Analytical Chemistry, Sos. Panduri, No. 90, Bucharest 050663, Romania*

† Electronic supplementary information (ESI) available. See DOI: 10.1039/c7ra10196a

isolate and concentrate these compounds from the initial sample. For instance, liquid–liquid extraction (LLE) and solid-phase extraction (SPE) are among the most utilized clean-up methods before analysis.[13–15] SPE is usually based on non-selective adsorbents,[16] but some examples of using molecularly imprinted polymers (MIPs) as selective adsorbents are also known for analyte isolation and enrichment.[17]

MIPs are polymeric matrices obtained using the so-called imprinting technology, which is based on the formation of a complex between an analyte (template) and a mixture of functional monomer a large excess of a cross-linking agent, when a three-dimensional polymer network is formed.[18] Usually, intermolecular interactions like H-bonds, dipole–dipole and ionic interactions between the template molecule and functional groups present in the polymer matrix drive the molecular recognition phenomena. Thus, the resultant polymer recognizes and binds selectively only the template molecules.[19,20] Up to the present, only a few MIPs for nitrofuran compounds were produced using monomers various functional moieties, such as (thio)urea,[21] methacrylamido pyridine[22] or a combination of a diaminopyridine and (thio)urea derivatives.[22] In this case, nitrofurantoin was efficiently bound by these MIPs, but also a broad spectrum of other nitrofurans were bound at intermediate levels and a detection method based on thermistor measurements allowed a limit of quantification of 1 ppm nitrofurantoin in acetonitrile.[23] The choice of monomer is very important in order to create highly specific cavities designed for the template molecule.

In this paper, we present new MIPs synthetized and applied for sample concentration and detection of furaltadone in aqueous samples. The monomers chosen in this study have not been used up to now for the synthesis of MIPs for nitrofuran templates and they are commercially available. The synthesis involved the free radical polymerization of selected monomers with the aim of obtaining hydrogen bonding with the template molecules. Their retention properties were studied using aqueous sample and various desorption solvents. For this purpose, the breakthrough curves were recorded and breakthrough parameters to estimate the adsorption properties were calculated. Their retention proved useful for application in selective SPE procedures of target analyte from aqueous samples and their determination by direct UV spectrometry. We describe also a method for the electrochemical detection of furaltadone using gold electrodes modified with MIPs immobilized by entrapment in sol–gel structures anchored with a SAM made with 3-mercaptopropyl trimethoxisilane and measurements carried out by electrochemical impedance spectroscopy (EIS).

Experimental

Materials

The monomers used for MIP synthesis: 2-hydroxyethyl methacrylate (HEMA) (Aldrich), acrylic acid (AA) (Aldrich), methacrylic acid (MAA) (Aldrich), *N*,*N*-diethylaminoethyl methacrylate (DEAEMA) (Aldrich), *N*-vinyl pyrrolidone (NVP) (Aldrich), *N*-vinyl carbazole (NVK) (Aldrich), acrylamide (AM) (Aldrich) are presented in Fig. 1. Also, the following cross-linking agents from Aldrich were employed in the reactions: ethylene glycol dimethacrylate (EGDMA) (Aldrich), *N*,*N*′-methylenebis(acrylamide) (MBA) (Aldrich) and triethyleneglycol dimethacrylate (TEGDMA) (Fig. 2).

The liquid monomers were passed through an alumina filled column in order to eliminate the inhibitors. NVK was purified by recrystallization from ethanol. The initiator 2,2′-azobis(2-methylpropionitrile) (AIBN) (Aldrich) was purified through recrystallization from methanol. The solvents (Merck) were used without any prior purification.

Synthesis

In a glass vial were introduced successively various quantities of monomers and cross-linker, 3 mL DMF and 80 mM template according to Tables 1 and 2. The mixture was stirred for 1 h prior to the addition of the initiator (AIBN – 2,2′-azobis(2-methylpropionitrile)) and was heated at 70 °C for 4 h. Blank experiments were performed in parallel in the absence of nitrofuran template to produce the corresponding non-imprinted polymers (NIPs).

The obtained imprinted polymers were washed with DMF and ethanol at the end of the reaction, filtered and dried. The

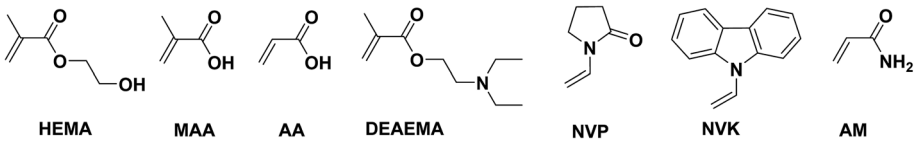

Fig. 1 Chemical structures of the monomers used.

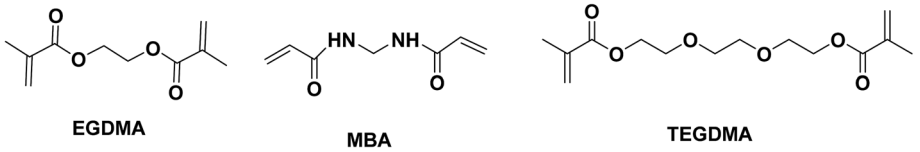

Fig. 2 Chemical structures of the cross-linking agents.

Table 1 Monomers amounts used for the synthesis of MIP/NIP for furaltadone

	MAA		DEAEMA		HEMA		NVK		NVP		EGDMA		MBA	
	g	mmol	g	mmol	g	mmol	g	mmol	g	mmol	g	mmol	g	mmol
MIP-F1	1.88	21.88	0.92	4.98	—	—	0.50	2.59	—	—	1.05	5.30	—	—
MIP-F2	1.25	14.59	0.92	4.98	—	—	0.50	2.59	0.52	4.68	1.05	5.30	—	—
MIP-F3	1.25	14.59	0.92	4.98	—	—	0.50	2.59	0.52	4.68	0.79	3.98	0.25	1.62
MIP-F4	1.25	14.59	0.46	2.49	2.15	16.49	—	—	—	—	—	—	0.10	0.65

Table 2 Monomers amounts used for the synthesis of MIP/NIP for nitrofurantoin

	AA		AM		HEMA		NVP		MBA		TEGDMA	
	g	mmol	g	mmol	g	mmol	g	mmol	g	mmol	g	mmol
MIP-N1	0.76	10.5	2.49	35	1.37	10.5	—	—	0.54	3.5	—	—
MIP-N2	1.44	20	2.84	39.97	0.52	4	—	—	0.62	4	—	—
MIP-N3	0.54	7.5	—	—	0.97	7.5	2.78	25	—	—	0.72	2.5
MIP-N4	1.08	15	—	—	0.39	3	3.33	30	—	—	0.86	3
MIP-N5	1.4	16.2	1.06	15	0.39	3	1.67	15	—	—	0.86	3

specific surface was increased through grinding followed by sieving to separate particles with sizes less than 70 μm.

The removal of the template was done by Soxhlet extraction using DMF (24 h) and water (12 h). After extraction, the polymers were dried until constant mass.

Characterization

The FT-IR (Fourier transform infrared spectroscopy) spectra were obtained using a Bruker VERTEX 70 Spectrometer with ATR (attenuated total reflection). Data were collected by averaging 32 scans, at a resolution of 4 cm^{-1}, from 500 to 4000 cm^{-1}.

The polymer particles morphology was also investigated using a scanning electron microscope, FEI Co. (model Inspect S), 0–30 kV accelerating voltage, working distance 0–30 mm, with ECON 4/6 EDAX, silicon (Li) energy dispersive detecting unit. Planar images have been recorded on different locations of the samples.

Thermogravimetric analysis (TGA) measurements were determinate using LABSYS EVO TG-DTA/DSC 1150 °C analyzer including: the thermally insulated TGA module with a sample capacity of 20 g max; measuring ranges: +/− 1000 mg or +/− 200 mg; electronic resolutions: 0.2 μg/0.02 μg; the connection module for simultaneous DTA or DSC measurement; the furnace with metallic resistor and temperature control thermocouple; temperature range: ambient up to 1150 °C max; temperature scanning rate: 0.01 to 100 °C min^{-1}.

SPE procedure

Retention properties of the synthetized polymers were investigated with the aid of an automated SPE HT400E system equipped with autosampler. The UV spectral measurements for various solutions involved in SPE processes were recorded with a Jasco V-530 double beam spectrometer, using 1 cm quartz cells, at room temperature.

An amount of 200 mg of the synthetized MIP/NIP was loaded on empty SPE cartridges. These cartridges were used in SPE procedures following the usual steps as indicated in Fig. ESI-1.† The aqueous sample was introduced in aliquots of 2.5 mL aqueous solutions containing 10 μg mL^{-1} of studied compounds (nitrofurantoin or furaltadone). The absorbance (A) of the eluate was measured at 365 nm, and the absorbance value was converted into concentration values, using the dependences between A and the concentration (C) of studied compounds. These dependences known as calibration equations are described by the following equations for: nitrofurantoin: $A = 0.0054 + 0.0379C$; and for furaltadone: $A = -0.0345 + 0.0519C$.

Immobilization of the MIP onto gold electrodes

Prior to modification, the gold electrode surface was cleaned by polishing with alumina (0.3 μm, Metrohm-Autolab), thoroughly rinsed with Milli-Q water and dried with argon. The sol–gel precursors were hydrolyzed overnight in acid solutions in order to transform the methoxy-silane moieties into hidroxy-silane functional groups that will polycondensate at neutral pH and form a matrix that immobilize the MIPs on the electrode surface. Two solutions were hydrolyzed overnight: solution (A) for formation of a self-assembled monolayer (SAM) prepared with 5 μL MPTS, 40 μL HCl 1 mM, 55 μL H_2O and solution (B) for formation of cage structure prepared with 5 μL MTMOS, 5 μL TMOS, 40 μL HCl 1 mM, 44 μL H_2O. The cleaned gold electrodes were immersed for 15 min in solution A diluted 400 times for SAM formation followed by thorough rising with distilled water and dried with an argon stream. On the electrode surface was gently deposed and spread 3 μL of a solution prepared from 25 μL solution B, 25 μL PBS and 4 mg de MIP-F3. The electrodes

were left at room temperature overnight for a complete polycondensation.

Measurement of nitrofurantoin using MIP-electrodes

Electrochemical impedance measurements were carried out using a PGSTAT302N potentiostat/galvanostat (Metrohm-Autolab) equipped with a conventional three-electrode cell in a Faraday cage and controlled using Nova 1.8 software. The working electrode was a gold electrode with 3 mm diameter from Metrohm-Autolab modified with MIPs using sol–gel, reference electrode was Ag/AgCl//3M KCl (Metrohm-Autolab) and platinum foil was used as an auxiliary electrode. The MIP-electrode was immersed for 15 min in PBS for hydration and surface stabilization and the impedance spectra corresponding to the baseline was recorded. Subsequently, the MIP-electrode was immersed for another 15 min in PBS and the impedance spectra were recorded again to confirm baseline stability due to unspecific electrode surface modification. The MIP-electrode was immersed for 10 min in stirred standard furaltadone solutions prepared in PBS and the impedance spectra was recorded to quantify the analytical signal associated with furaltadone. The MIP-electrode was regenerated by immersion for 10 min in ethanol and 10 min in PBS, followed the measurement of the impedance spectra to confirm the signal decrease to the baseline (complete removal of adsorbed furaltadone). The potentiostatic electrochemical impedance spectra measurements were made in PBS containing 1 mM ferri/ferrocyanide in equimolar ratio at open circuit potential (0.227 V) with a superposed alternative amplitude of 5 mV (rms). Impedance spectra were recorded for 40 frequencies logarithmically distributed between the frequency range 9.5 kHz and 0.1 Hz. The results were represented as Nyquist plots and interpolated using Randles equivalent circuit where R_s is the electrolyte resistance, R_{ct} is the charge transfer resistance at the electrode interface, Q is the constant phase element related to the double layer capacitance, W is the Warburg impedance used to simulate the mass-transport effects in solution bulk. The variation of the charge transfer resistance (ΔR_{ct}) was used for the surface characterization and correlated with the concentration of furaltadone from the sample solution.

Results and discussion

Synthesis and characterization

The first stage of our study consisted in the monomer selection capable of forming hydrogen bonds with the template molecules. In order to highlight the possible interactions different molar ratio between the monomers were used. The possible routes for hydrogen bonds formation between the monomers and the template molecule are presented in Fig. 3A. Further hydrogen bonds interactions are also possible to include the cross-linking agents and the template molecule (see Fig. 3B). This aims at increasing the retention capacity of the final imprinted polymer. Another monomer–template interaction that was envisaged involved the free electrons of the nitrogen atoms from the monomer, capable to interact with the electron accepting nitro groups of the template, as well as π–π stacking between the furan rings and the aromatic molecules of the monomer (Fig. 3C). In contrast to literature examples,[21–23] our MIPs design utilizes commercially available monomers and does not require complex synthesis of highly functional monomers. This strategy was adopted to facilitate a possible scale-up of the process at an affordable cost.

In order to investigate the interaction between the template the polymer, the FT-IR spectra for the MIP-F3 and its corresponding non-imprinted polymer are presented in Fig. ESI-2.† A decrease of the maximum intensity can be observed in the case of the imprinted polymer for the signal characteristic to the vibrations of C–O (ν_{C-O} 1160 cm^{-1} and 1380 cm^{-1}), C=O ($\nu_{C=O}$ 1660 cm^{-1} and 1720 cm^{-1}), C–N (ν_{C-N} 2950 cm^{-1}) or O–H (ν_{O-H} 3380 cm^{-1}) as well as a slight shift of the values between the imprinted and non-imprinted sample.

The morphology analysis of MIP-F3, through SEM analysis, revealed large polymer aggregates with a maximum size of 70 μm (Fig. ESI-3†). Due to the bulk polymerization procedure employed and random cross-linking of the polymer, the grinding process afforded irregular shapes and sizes for the imprinted polymers. Similar characteristics can be observed in the case of MIP-N3, the images being presented in the ESI (Fig. ESI-4†).

The thermal behavior of the polymers is one of their most important property. Thus, TGA analysis of the imprinted polymer MIP-F3 with furaltadone, MIP-F3 after furaltadone removal and furaltadone are presented in Fig. 4A. In the case of MIP-F3 with furaltadone several decomposition steps can be observed of which the one at 260 °C corresponds to the decomposition of furaltadone and the polymer decomposition at 440 °C. The thermal decomposition of MIP-F3 with furaltadone has multiple steps due to the physical interaction between furaltadone and the polymer that has to be disrupted. A similar behavior can be observed for the sample set comprised of MIP-N3 with nitrofurantoin, MIP-N3 after removal of nitrofurantoin and nitrofurantoin (see Fig. 4B).

Retention properties – elution curves and breakthrough parameters

The retention capacity of each synthetized MIP/NIP was studied according to the usual SPE procedure, mentioned in Experimental section. This capacity is described by the elution curve, which represents the dependence of eluate concentration for consecutive volume of aqueous samples loaded on the cartridge containing 200 mg of each synthetized adsorbent. An ideal shape of such curve is sigmoidal one, described by Boltzmann's function, as depicted in Fig. 5A. Examples of such curves obtained for three synthetized MIPs for furaltadone and nitrofurantoin are depicted in Fig. 5B and C, respectively. As a remark, the SPE elution process was made with difficulty for another synthetized MIP, encoded by MIP-F4, whose elution curve was not available. However, the experimental curves deviate from the theoretical shape, but they prove the adsorption behavior of these polymers. Thus, as can be seen from this figure, the MIPs designed for furaltadone showed a double

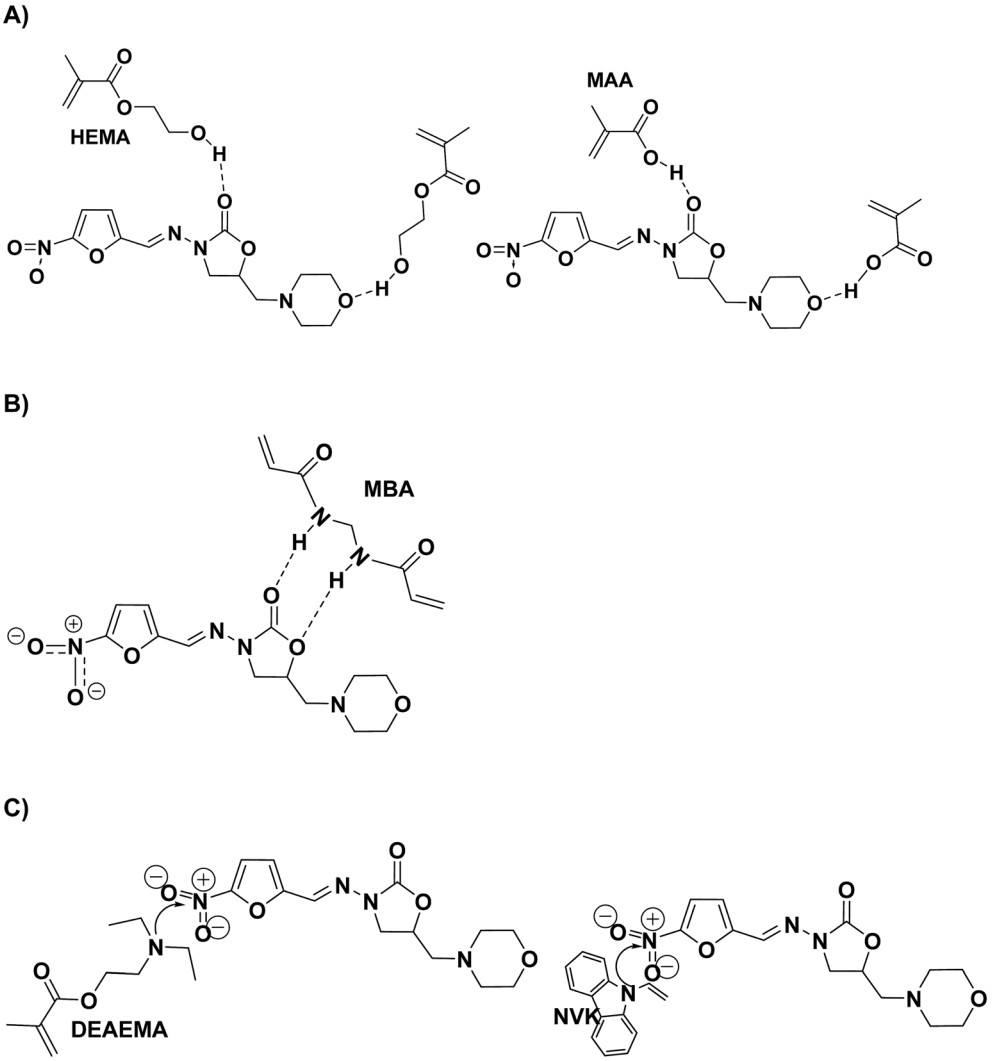

Fig. 3 Interactions between the furaltadone template and components used for synthesis of MIP: (A) hydrogen bonds formation between the template and monomers, (B) cross-linker capacity to form hydrogen bonds with the template and (C) other possible interaction based on electron transfer interactions.

sigmoid shape, which is characteristic to the retention mechanism based on double retention mechanism of analyte on the surface of adsorbent. Unlike MIPs for furaltadone, the MIPs designed for nitrofurantoin showed breakthrough curves described by a single sigmoid shape, which corresponds to a unique retention mechanism of this compound from aqueous solutions. Not shown in these figures, the curves corresponding to the SPE study applied in the same conditions on NIPs presented only the final plateau, leading to the conclusion they have no retention property toward these compounds. A real problem given by the leakage of a template molecule from the MIP bed[24] was also checked by applying volumes of 5 mL of methanol on the cardtriges loaded with MIP (first step of the SPE procedure, namely cartridge conditioning, indicated in Fig. ESI-1†), and measuring the absorbance at 365 nm, which was each time very close to 0 (lack of template compound in eluate solvent).

The analysis of the elution curves and the values of its parameters, as given below, revealed that they have similar retention properties for the target compounds. The retention parameters characterizing the SPE procedures using the synthetized NIPs and MIPs can be estimated with the aid of three characteristic points of the sigmoid shape breakthrough curve, as illustrated in Fig. 5A:[25,26]

- V_B point represents the breakthrough volume, corresponding to a value of 1% of maximum concentration of the analyte found in eluate; this parameter typically indicates the volume that can be loaded on the adsorbent bed with no loose of the solutes;

- V_R point represents the retention volume (given by the inflection point of retention curve), where the solute adsorption is in equilibrium with desorption from sorbent bed;

- V_M point represents the hold-up volume (maximum), which corresponds to the volume at which analyte concentration entering and exiting the cartridge is the same.

The experimental breakthrough curves obtained for studied compounds given in Fig. 4B and C, can be fitted by means of Boltzmann's function (containing A_1, A_2, x_0 and dx as regression parameters), written as following:[27]

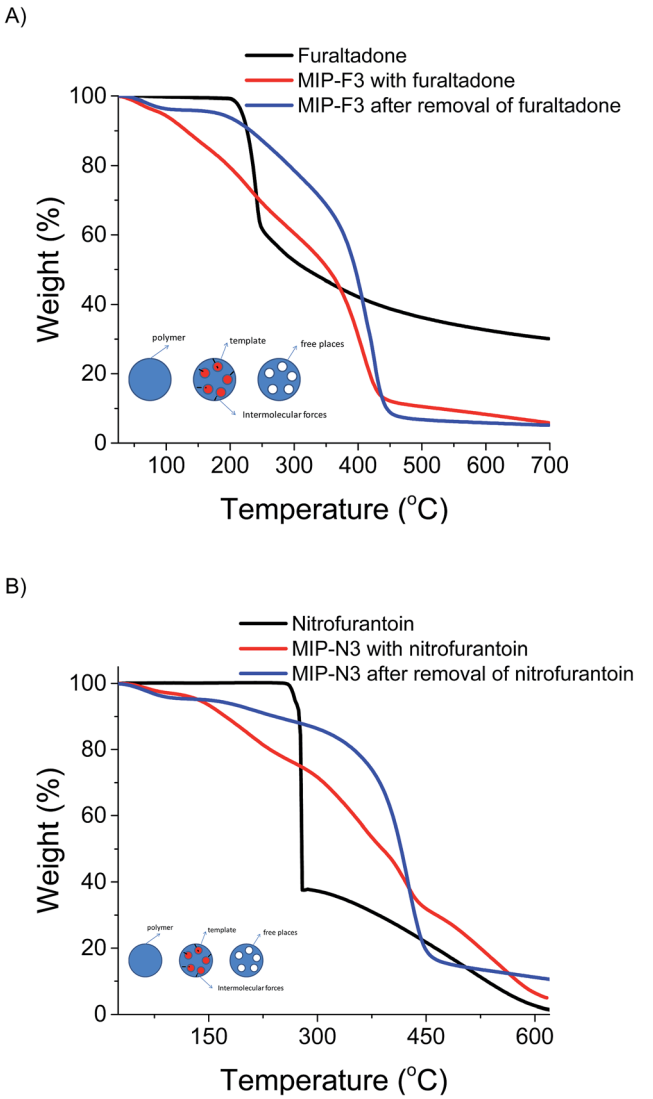

Fig. 4 Thermogravimetric analysis (TGA) for the synthetized MIPs. (A) MIP-F3 with furaltadone, MIP-F3 after removal of furaltadone and furaltadone; (B) MIP-N3 with nitrofurantoin, MIP-N3 after removal of nitrofurantoin and nitrofurantoin.

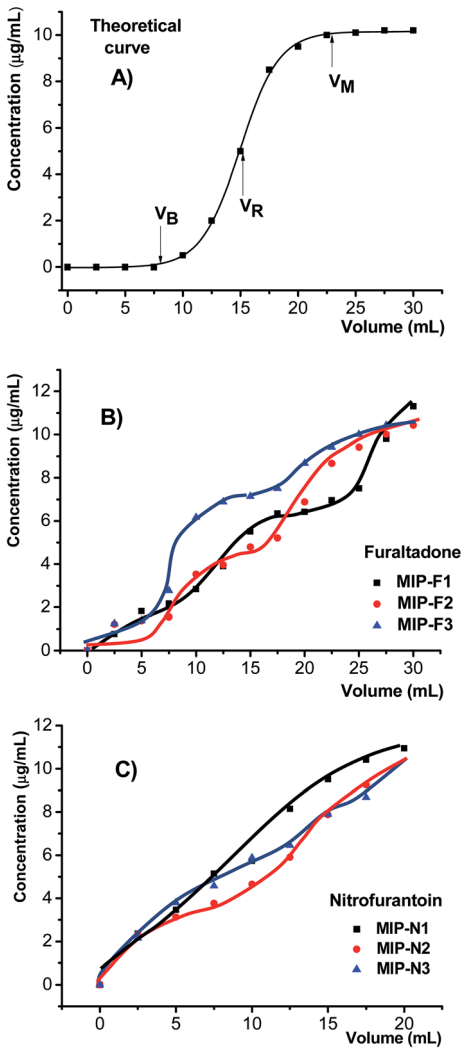

Fig. 5 Breakthrough curves obtained for three synthetized MIPs, obtained from SPE procedure using these adsorbents. (A) A theoretical curve for comparison, (B) the curves for furaltadone and (C) the curves for nitrofurantoin.

$$Y = A_2 + \frac{A_1 - A_2}{1 + e^{\frac{x - x_0}{dx}}} \quad (1)$$

where Y represents the measured concentration of analyte in eluate, x – the volume of liquid sample loaded on the sorbent bed.

This equation can be used in calculating the value of V_B, V_R, V_M values according to the following relationships:[27]

$$V_B = x_0 + (dx)\ln\left[\frac{100}{99}\left(1 - \frac{A_1}{A_2}\right) - 1\right] \quad (2)$$

$$V_M = x_0 + (dx)\ln\left(99 - 100\frac{A_1}{A_2}\right) \quad (3)$$

$$V_R = x_0 \quad (4)$$

The calculated values of these parameters for three MIPs adsorbents for each template compound given as examples are given in Table 3. These values are similar to other synthetized and reported sorbents in SPE procedures.[28] Due to the fact that the NIPs showed no retention property towards these compounds, the values of these retention parameters are 0. Experimentally, it was observed that the curves obtained for NIPs reached the maximum ($V_M = 0$) at the first solution applied to the loaded cartridge with these polymers, proving that these types of adsorbents do not retain the template molecule during the SPE procedure.

The elution curves and their calculated breakthrough parameters pointed out clear retention property of the synthetized adsorbents, and therefore can be used in analytical procedures for sample enrichment and analyte isolation from liquid samples. For example, knowing the concentration of the initial solution furaltadone of 10 μg mL^{-1}, its molecular weight (M_w) of 324.29 g mol^{-1} and the adsorbent amount loaded onto

Table 3 Computed values of the SPE procedure (results are expressed in mL solution of 10 ppm analyte)

Compound	Sorbent	V_B	V_R	V_M
Furaltadone	MIP-F1	4.5	9	15
	MIP-F2	4.2	9.3	14
	MIP-F3	4.3	8.4	13
	MIP-F4	—	—	—
Nitrofurantoin	MIP-N1	0	7.5	20
	MIP-N2	0	8	18
	MIP-N3	0	7.5	18
	MIP-N4	—	—	—
	MIP-N5	—	—	—

the cartridge (200 mg MIP), we calculated the retention capacity of various synthetized adsorbents as being situated within the interval of 3.85–4.65 μmol g^{-1}. For nitrofurantoin (M_w = 238.16 g mol^{-1}), the retention capacities of the corresponding MIPs were calculated as varying within the interval 3–6 μmol g^{-1}. Considering a ten-times enrichment procedure applied then for furaltadone at lower concentration followed the following procedure: 20 mL of aqueous samples volume at the concentration levels (0.125; 0.25; 0.50; 1; 2 μg mL^{-1} furaltadone) were loaded on individual cartridges containing 200 mg MIP and then the analytes were eluted with 2 mL of methanol. The absorbance of the final solutions was measured at 365 nm. The calibration curve for furaltadone was described by the regression: $A = 0.0171 + 0.4204C_{furaltadone}$ (where C was given in μg mL^{-1}); the regression coefficient r^2 being 0.9975. Comparing the slope of the calibration curve (0.4204) with that obtained by procedure that does not use MIP enrichment (0.0519), mentioned in Experimental section, we can calculate a practical enrichment factor of 8.1. For nitrofurantoin, the same ten-times enrichment procedure leads to a calibration curve described by the regression equation: $A = 0.0061 + 0.3221C_{nitrofurantoin}$ (r^2 = 0.9961), with a practical enrichment factor of 8.5.

Selectivity was checked by applying the entire SPE procedure based on synthetized MIPs for some possible interferences due to AOZ, AMOZ, SEM or AHD (mentioned in Introduction), which showed that these species are not retained in the cavities of sorbent bed, probable due to their smaller molecular dimensions compared to the template molecules used to synthetize these MIPs.

MIP-electrode for furaltadone

The stable immobilization of the MIP on the electrode surface was achieved by MIP entrapment in a sol–gel cage like structure. In order to assure a good mechanical linkage between the electrode surface and the sol–gel layer it was formed a SAM using MPTS (an organosilane that has also a thiol moiety with affinity for gold surface) according to the Fig. 6. The sol–gel layer deposed on the gold electrode in the absence of the SAM does not have a good mechanical adherence and has the tendency to peel off. We have observed that SAM has passivating properties that impede the electrochemical charge transfer and implicitly negatively affects the furaltadone detection by electrochemical impedance measurements. Thus, we have optimized the SAM formation in order to achieve a good stability of the sol–gel layer (provided by a dense SAM) concomitant with a suitable resistance to charge transfer (sparse SAM). Two parameters were optimized for the SAM formation: dilution of the MPTS solution (1/20, 1/200 and 1/400) and the electrode

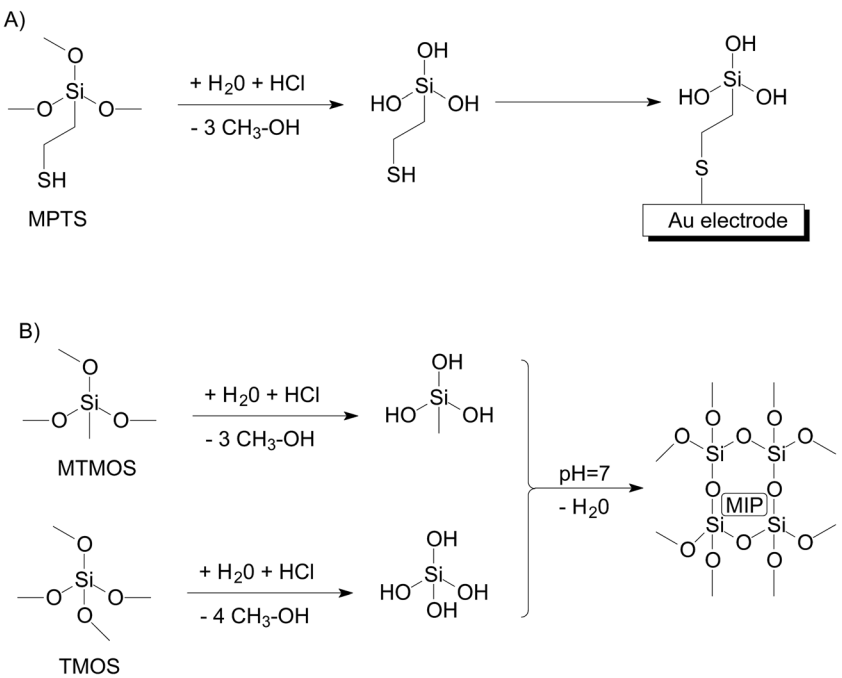

Fig. 6 The schematic representation of the MIP immobilization on the gold electrode surface by entrapment in sol–gel matrix. (A) Hydrolysis of the MPTS followed by SAM formation. (B) Hydrolysis of MTMOS and TMOS followed by sol–gel structure formation around the MIP particles. Note: the structure depicted in (B) is anchored on the electrode surface *via* the links of the SAM from (A).

immersion time (1 hour, 30 min and 15 min). We have observed that measured R_{ct} values greatly decreases for higher MPTS dilution and/or shorter SAM formation times, *e.g.* the R_{ct} is 333 kΩ for SAM formation during 15 min in a diluted solution 1/20, 19.1 kΩ for SAM formation during 1 hour in a diluted solution 1/200 or 2.1 kΩ for SAM formation during 15 min in a diluted solution 1/400. We have considered that an optimum SAM was obtained with a deposition time of 15 min using MPTS solution diluted 1/400.

The MIP-electrode has a good operational stability and the recorded analytical signals are reproducible. The stability of the MIP-electrode was verified by recording 20 successive measurements of the electrochemical impedance separated by MIP-electrode washing and immersion in PBS. The relative standard deviation of the R_{ct} corresponding to the baseline signal is 10% ($R_{ct} = 4.6 \pm 0.46$ kΩ; $n = 20$). The R_{ct} values measured after the MIP-electrode washing with ethanol and PBS following furaltadone analysis are also similar to the initial baseline values. Thus, we have concluded that the MIP-electrodes may be used for multiple analyses based on their good stability and regeneration possibility. The MIP-electrodes were tested using standard furaltadone solutions with concentrations of 0.01, 0.1 and 1 ppm. The ΔR_{ct} values are directly correlated with the furaltadone concentration and thus we have demonstrated the possibility to develop a fast sensor for furaltadone analysis. From the few MIPs developed for nitrofuran compounds that were previously published,[21–23] only one was study reported the development of an analytical method based on thermistor measurements with the MIP inserted in a column.[23] The reported detection method achieved a limit of quantification of 1 ppm nitrofurantoin in acetonitrile,[23] a concentration level that is significantly higher in comparison with our impedimetric sensors.

Conclusions

MIPs based commercial monomers capable of interaction with nitrofuran antibiotics were synthesized through free-radical polymerization. The synthetized MIPs exhibited retention properties towards the template compounds and this property were utilized in solid-phase procedures applied to aqueous solutions at low concentration of studied compounds. Both synthetized MIPs, for furaltadone and nitrofurantoin, showed selective adsorption properties for these compounds, and analytical procedures can be developed using these sorbents for their concentration from aqueous samples. Interestingly, we have also demonstrated the possibility to develop impedimetric sensors based on MIPs that were immobilized on gold electrodes by entrapment in a silane sol–gel matrix. The sol–gel matrix was immobilized in a stable manner on the gold surface using a SAM based on 3-mercaptopropyl trimethoxisilane, a compound that has affinity for gold surfaces provided by its thiol moieties and can bind to the sol–gel structure through the hydrolysis of the methoxy-silane groups.

Conflicts of interest

There are no conflicts to declare.

Acknowledgements

The authors acknowledge the financial support of this work by the Romanian Department of Education and Research (MEN-UEFISCDI) projects PN-III-P2-2.1-PED-2016-0503 and PN-II-PT-PCCA-2013-4-0203.

References

1 M. Vass, K. Hruska and M. Franek, *Vet. Med.*, 2008, **53**, 469.
2 M. M. Vasheghani, M. Bayat, F. Rezaei, A. Bayat and M. Karimipour, *Photomed. Laser Surg.*, 2008, **26**, 1.
3 G. H. Rabbani, T. Butler, M. Shahrier, R. Mazumdar and M. R. Islam, *Antimicrob. Agents Chemother.*, 1991, **35**, 1864.
4 W. A. Petri Jr, *Trends Parasitol.*, 2003, **19**, 523.
5 D. R. Guay, *Drugs*, 2008, **68**, 1169.
6 K. M. Cooper, R. J. McCracken, M. Buurman and D. G. Kennedy, *Food Addit. Contam., Part A: Chem., Anal., Control, Exposure Risk Assess.*, 2008, **25**, 548.
7 EFSA Panel on Contaminants in the Food Chain (CONTAM), Scientific Opinion on nitrofurans and their metabolites in food, *EFSA J.*, 2015, **13**(6), DOI: 10.2903/j.efsa.2015.4140.
8 http://webgate.ec.europa.eu/rasff-window/portal/index.cfm?event=searchResultList,researchsubject=nitrofuran.
9 H. An, M. Henry, T. Cain, B. Tran, H. C. Paek and D. Farley, *J. AOAC Int.*, 2012, **95**, 1222.
10 C. A. Lázaro de la Torre, J. E. Blanco, J. T. Silva, V. M. F. Paschoalin and C. A. Conte Júnior, *Arq. Inst. Biol., Sao Paulo*, 2015, **82**, 1.
11 Q. Zhang and Y. Ni, *RSC Adv.*, 2017, **7**, 39833.
12 W. M. A. Niessen, *J. Chromatogr. A*, 1998, **812**, 53.
13 J. Wang, *Mass Spectrom. Rev.*, 2009, **28**, 50.
14 R. J. McCracken and D. G. Kennedy, *Food Addit. Contam.*, 2007, **24**, 26.
15 S. Bogialli and A. Di Corcia, *Anal. Bioanal. Chem.*, 2009, **395**, 947.
16 R. J. McCracken, W. J. Blanchflower, C. Rowan, M. A. McCoy and D. G. Kennedy, *Analyst*, 1995, **120**, 2347.
17 X. Song, S. Fu, L. Chen, Y. Wei and H. Xiong, *J. Appl. Polym. Sci.*, 2014, **131**, 40766, DOI: 10.1002/app.40766.
18 M. Lasakova and P. Jandera, *J. Sep. Sci.*, 2009, **32**, 799.
19 G. Vasapollo, R. Del Sole, L. Mergola, M. R. Lazzoi, A. Scardino, S. Scorrano and M. Giuseppe, *Int. J. Mol. Sci.*, 2011, **12**, 5908.
20 K. Haupt and K. Mosbach, *Chem. Rev.*, 2000, **100**, 2495.
21 U. Athikomrattanakul, M. Katterle, N. Gajovic-Eichelmann and F. W. Scheller, *Talanta*, 2011, **84**, 274.
22 U. Athikomrattanakul, M. Katterle, N. Gajovic-Eichelmann and F. W. Scheller, *Biosens. Bioelectron.*, 2009, **25**, 82.
23 U. Athikomrattanakul, N. Gajovic-Eichelmann and F. W. Scheller, *Anal. Chem.*, 2011, **83**, 7704.
24 J. Haginaka, *J. Sep. Sci.*, 2009, **32**, 1548.

25 K. Bielicka-Daszkiewicz and A. Voelkel, *Talanta*, 2009, **80**, 614.
26 K. Bielicka-Daszkiewicz, *J. Liq. Chromatogr. Relat. Technol.*, 2016, **39**, 477.
27 E. Bacalum, M. Radulescu, E. E. Iorgulescu and V. David, *Rev. Roum. Chim.*, 2011, **56**, 137.
28 M. Iacono, D. Connolly and A. Heise, *RSC Adv.*, 2017, **7**, 19976.